Supplementary information

Non-thermal Pulsed Plasma Activated Water: Environmentally Friendly Way for Efficient Surface Modification of Semiconductor Nanoparticles

Pavel Galář*[a], Josef Khun[b], Anna Fučíková[c], Kateřina Dohnalová[d], Tomáš Popelář[a], Irena Matulková[e], Jan Valenta[c], Vladimír Scholtz[b] and Kateřina Kůsová[a]

*E-mail of corresponding author: galar@fzu.cz

Influence of specific atmospheres on PL change of PAW modified Si-NCs

To verify our statement that PAWs of low or no concentration of hydrogen peroxide and a simultaneous high concentration of other reactive species has a beneficial effect on the nanoparticle surface chemistry, we measured PL spectra of Si-NCs A dispersed in the water before and after its activation under closed atmospheres of oxygen, nitrogen and air (**Figure S6**, chemical analysis **Table S1**). We have observed that while the PL of Si-NCs changed only negligibly after the modification at oxygen, the PL of a sample modified at nitrogen and standard air atmosphere rose 2 times and 2.6 times, respectively. This results are well correlated with the concentration of hydrogen peroxide and nitrite and nitrate ions in the PAW (**Table S1**).

Modification of fresh Si-NCs using corona discharge pre-treatment

It is well known that surface chemistry of freshly electrochemically etched Si-NCs is not stable after its preparation. It commonly needs several days to reach optimal surface stabilization which is manifested by the blue shift of PL and an increase of QY. These processes are connected with the oxygen-related surface passivation, in particular a change of the initial hydrogen termination.[1,2] To determine the effect of PAW on different/early-stage surface chemistry of Si-NCs, we compared the PAW modification of nanocrystals with an already stable surface and the freshly prepared ones (**Figure 6a,b**). Surprisingly, we observed only low effect of PAW modification on the PL properties of "fresh" Si-NCs. This phenomenon can be interpreted taking into account the wide range of reactive species in PAW and the high reactivity of "fresh" Si-NCs.[2,3] While only the strongest modification processes can be take place in a surface modification of stable Si-NCs, in the case of the "fresh" Si-NCs, even the weaker and often mutually competitive processes can be involved, which results in a negligible improvement of sample passivation and the associated QY. To verify this assumption, we tried to homogenize the surface chemistry of the "fresh" Si-NCs and modify it by PAW afterwards. For this purpose we exposed the dried "fresh" Si-NCs powder to the standard corona discharge. In contrast to the pulsed transient spark discharge, the corona discharge is a much weaker modification medium and thus has a good prerequisite for a gentle surface pre-treatment. Apparatus was assembled according to **Figure S1a**. The stream of active species from a plasma jet were directed against the sample and to achieve homogenous exposure additionally scattered by metal grating. Moreover, to increase the modification effect, the sample and both electrodes were places into a confined space. The passing current of the discharge was set to 0.2 mA and the modification took place for 4 hours. The modified sample was dispersed in water and modified by PAW in the presence of the transient spark discharge. The effect of the corona pre-treatment manifested itself in several ways. First of all, the pre-treated Si-NCs showed a red spectral shift of the PL maximum from approximately 740 to 760 nm. Secondly, in contrast to the non-pre-treated sample, during the PAW activation we observed a significant increase of PL, which reached up to a 6.3 times. This enhancement valve is significantly higher than any of our attempts on stable Si-NCs (**Figure S5b**). Even though the PL spectra of the sample started to shift from 760 nm that the resulting PAW modified spectra finished at about 708 nm, which is in agreement with the modification of stable Si-NCs. However, the obtained intensities are not that stable as we saw in stable Si-NCs. We observed

a decrease of this improved PL by approximately 40 % in 7 days (to a 3.6 times increase with respect to the initial state) (**Figure S10**). A further decrease of PL intensity was not observed. To study the progression of the Si-NCs corona pre-treatment, we have PAW-modified nanocrystals which were kept in standard ambient conditions for 2 days after the pre-treatment (**Figure S10**). Even in this case the Si-NCs showed an increase in the PL intensity of a magnitude of 3.1 times with respect to the initial value and a blue spectral shift. Surprisingly, the corona discharge pre-treatment has no effect on stable Si-NCs. Modifications realized on stable Si-NCs showed a similar PL rise as without the pre-treatment.

Influence of PAW environment on the PL properties of modified Si-NCs

The presented physical properties of PAW modified Si-NCs can be influenced not only by their surface modification, but also by the presence of the radicals increasing the conductivity of the dispersion and lowering its pH to about 1.5 - 2.[4] To elucidate the influence of these effects on the PAW modified samples, we modified Si-NCs by PAW, split the dispersion into two parts and purified one part using dialysis tubing (Sigma-Aldrich, cellulose tubing, 23 mm, MWCO 12400). The modified Si-NCs were retained in the purified colloid, but > 99 % of the nitrogen-related radical species were removed. While the purified sample showed neutral pH, it kept the same PL response and dispersibility as in before the purification (**Figure S9**), thus, the changes of the physical properties of the PAW-modified Si-NCs are caused by the surface modification and not only by pH of the environment. The good dispersibility of the modified Si-NCs in the purified water was also verified by zeta potential measurements, showing the value of (-46 ± 2.8) mV.

References

1 Dohnalová, K., Kůsová K., Pelant I. Time-resolved photoluminescence spectroscopy of the initial oxidation stage of small silicon nanocrystals. *Appl. Phys. Lett.*, 2009, **94**(21), 211903, doi: 10.1063/1.3141481.

2 Sailor, M. J., Lee E. J. Surface chemistry of Luminescent Silicon Nanocrystallites. *Adv. Mater.*, 1997, **9**(10), 783-93, doi: 10.1002/adma.19970091004.

3 Bruggeman, P. J., Kushner M. J., Locke B. R., Gardeniers J. G. E., Graham W. G., Graves D. B., Hofman-Caris R. C. H. M., Maric D., Reid J. P., Ceriani E., Fernandez Rivas D., Foster J. E., Garrick S. C., Gorbanev Y., Hamaguchi S., Iza F., Jablonowski H., Klimova E., Kolb J., Krcma F., Lukes P., Machala Z., Marinov I., Mariotti D., Mededovic Thagard S., Minakata D., Neyts E. C., Pawlat J., Petrovic Z. L., Pflieger R., Reuter S., Schram D. C., Schröter S., Shiraiwa M., Tarabová B., Tsai P. A., Verlet J. R. R., von Woedtke T., Wilson K. R., Yasui K., Zvereva G. Plasma–liquid interactions: a review and roadmap. *Plasma Sources Sci. Technol.*, 2016, **25**(5), 053002, doi: 10.1088/0963-0252/25/5/053002.

4 Cannas, M., Camarda, P., Vaccaro, L., Amato, F., Messina, F., Fiore, T. and Li Vigni, M. Enhancing the luminescence efficiency of silicon-nanocrystals by interaction with H^+ ions. *Phys. Chem. Chem. Phys.*, 2018, **20**, 10445-10449, doi: 10.1039/c8cp00616d.

Figures and Tables

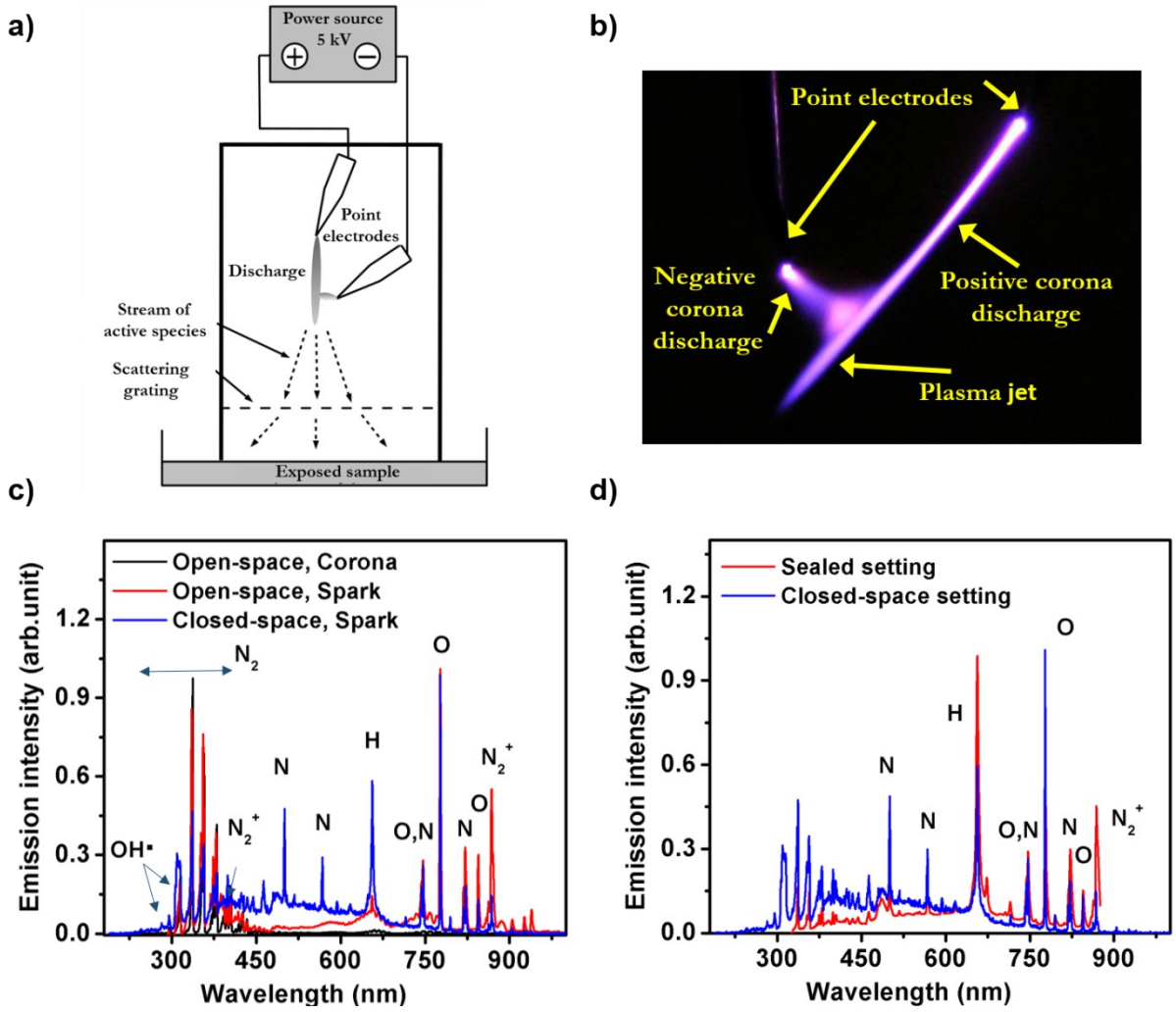

Figure S1. a) Scheme of the apparatus for the corona discharge generation. b) Picture of corona discharge and the generated plasma jet. c) Comparison of normalized emission spectra of the corona and the transient spark discharges using open-space and closed-space settings. The separated spectra are presented at **Figure 1c.** d) Comparison of the normalized emission spectra of the transient spark discharge using Sealed (standard air atmosphere) and closed-space settings. Discharges were generated at standard conditions: room temperature and atmospheric pressure. Emission spectra were obtained after the stabilization of the plasma discharge, which was approximately 5 minutes. The origin of the main peaks is indicated.

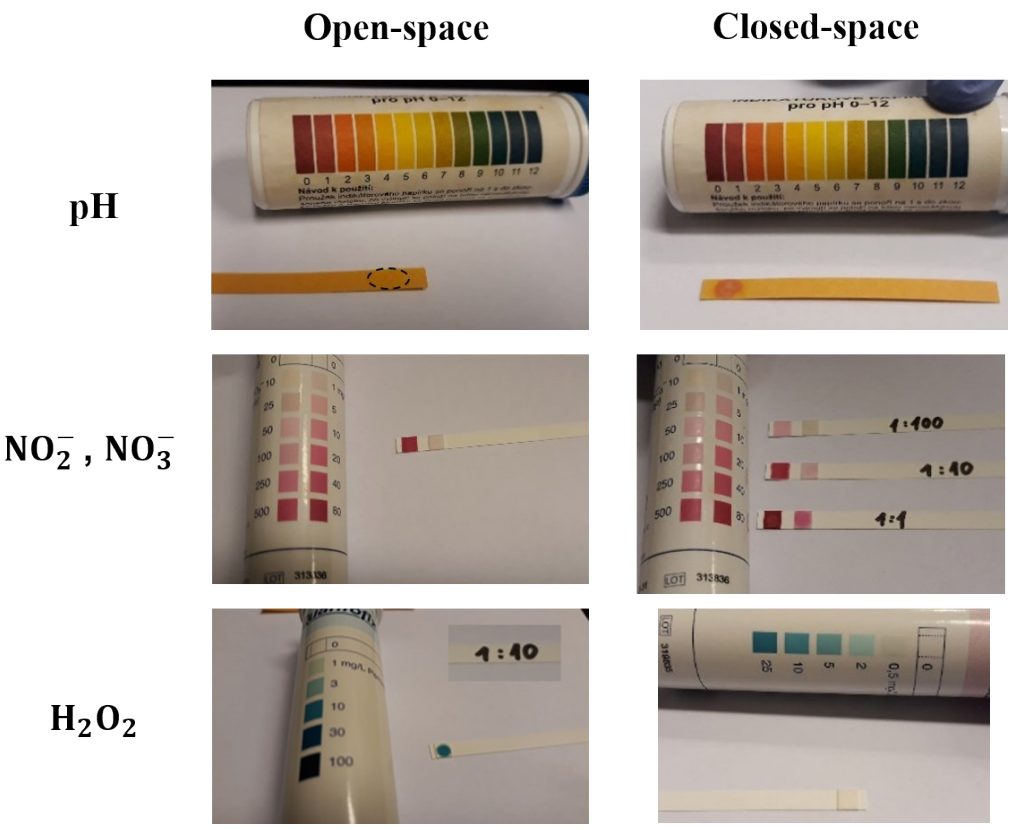

Figure S2. Photos of the test strips used for chemical ff plasma activated water prepared using opened- and closed-space setting. We monitored the following parameters of the PAW: pH, concentration of NO_2 and NO_3 anions and hydrogen peroxide. Expected error of the measurements is 20 %.

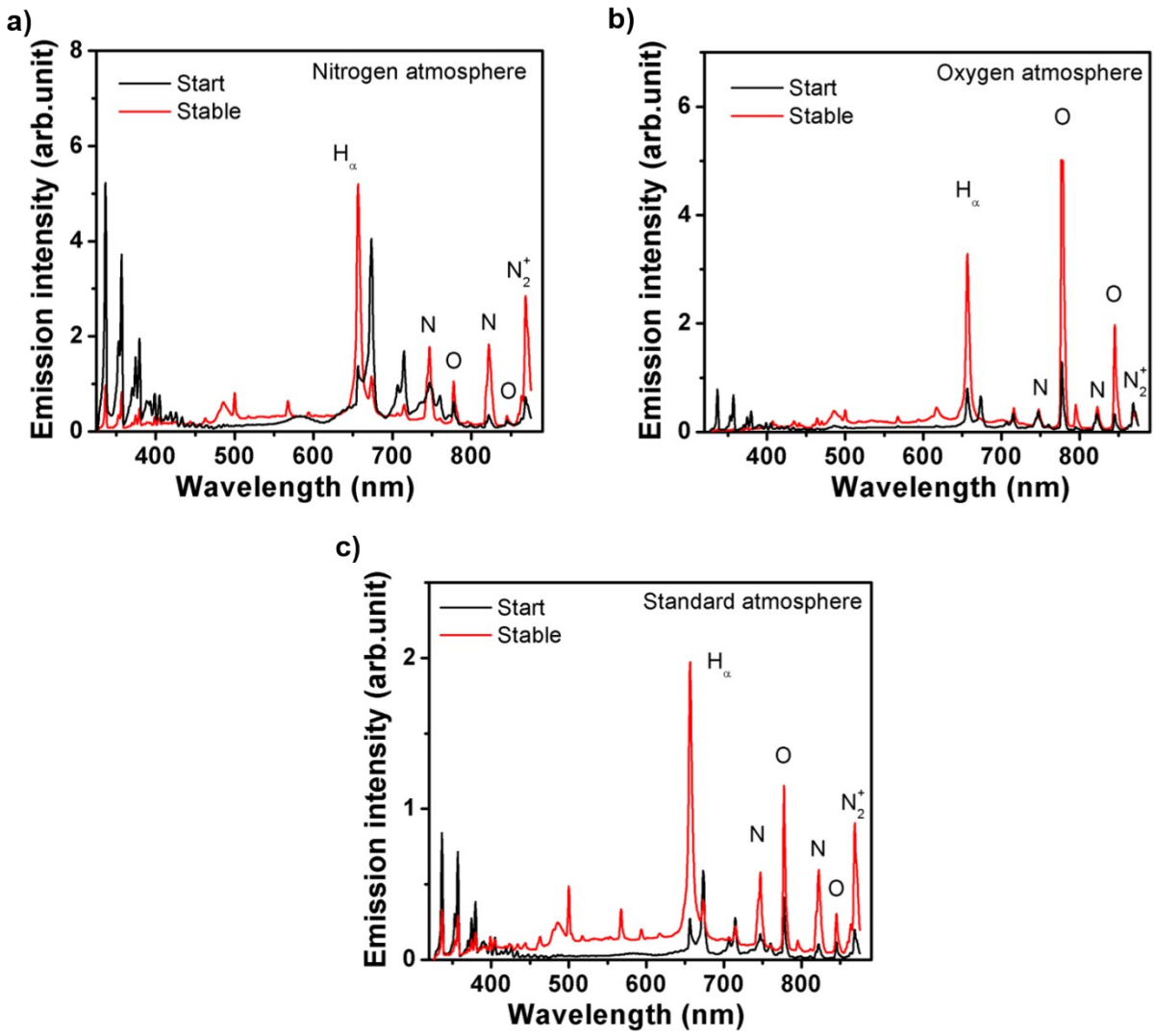

Figure S3. Comparison of the emission spectra of the transient spark discharge generated between a point electrode and the water level in closed a) nitrogen, b) oxygen and c) standard atmosphere at the beginning of the PAW modification and after reaching a stable state of the non-thermal plasma using the sealed setting. The conditions were optimized to gain comparable current through the discharge for both setting (approximately ~0.5 mA). The origin of the main peaks is indicated.

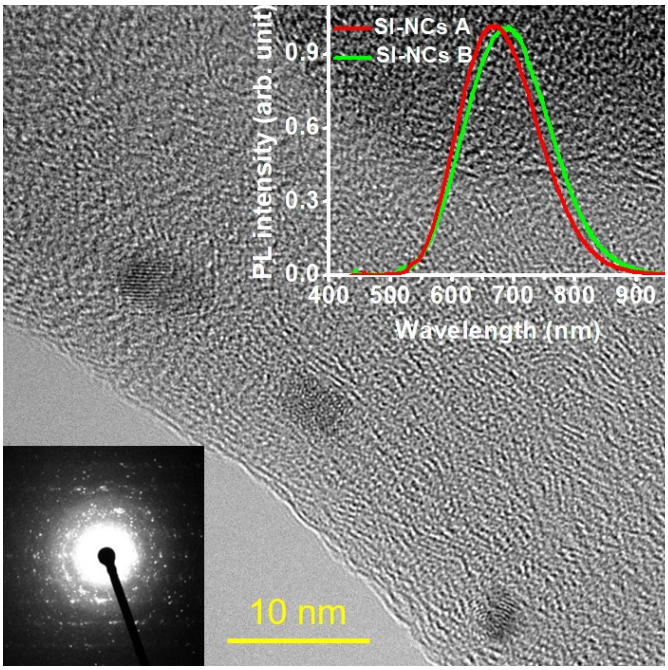

Figure S4. HRTEM image of Si-NCs prepared by wet electrochemical etching. Nanocrystals were separated into two samples according to their size. Time integrated photoluminescence spectra of both samples (A – smaller, B – Bigger) is presented by the inset (up right). The PL was excited by a continuous laser at 442 nm and intensity of 2.7 mW. The spectra are corrected for the spectral sensitivity of the detection setup. The second inset (down left) presents electron diffraction pattern of the displayed area.

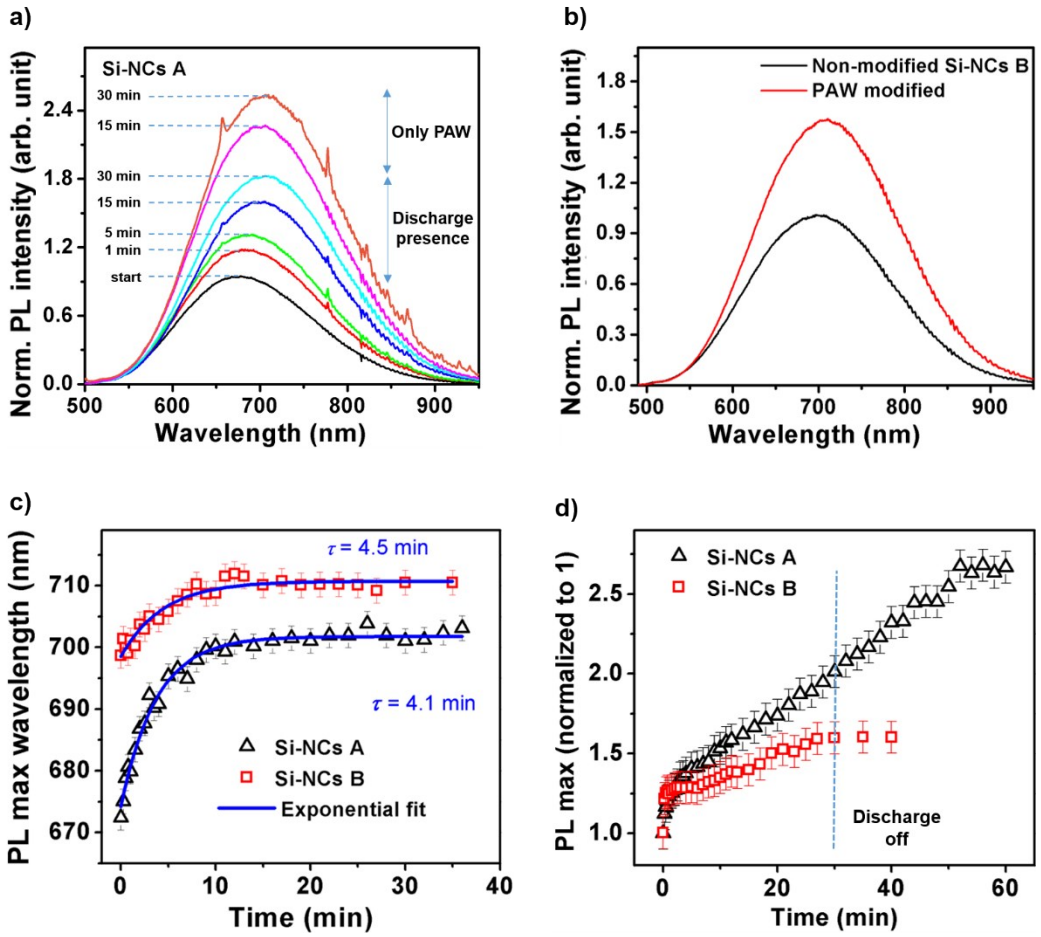

Figure S5. a) Temporal evolution of the PL spectra of the sample Si-NCs A during the first 30 minutes of the direct plasma modification of the water (method M2) and the following 30 minutes in the absence of the discharge (only PAW modification). b) Photoluminescence spectra of the sample Si-NCs B before and after PAW modification. Temporal evolution of the photoluminescence c) spectral position of the band maximum and d) maximal intensity of samples Si-NCs A and B during (30 minutes) and after PAW activation. Data are approximated by a single exponential curve. The resulting time constants are displayed. Photoluminescence was excited at 442 nm by a continuous beam of 2.7 mW. All spectra are corrected for the sensitivity of the whole detection system.

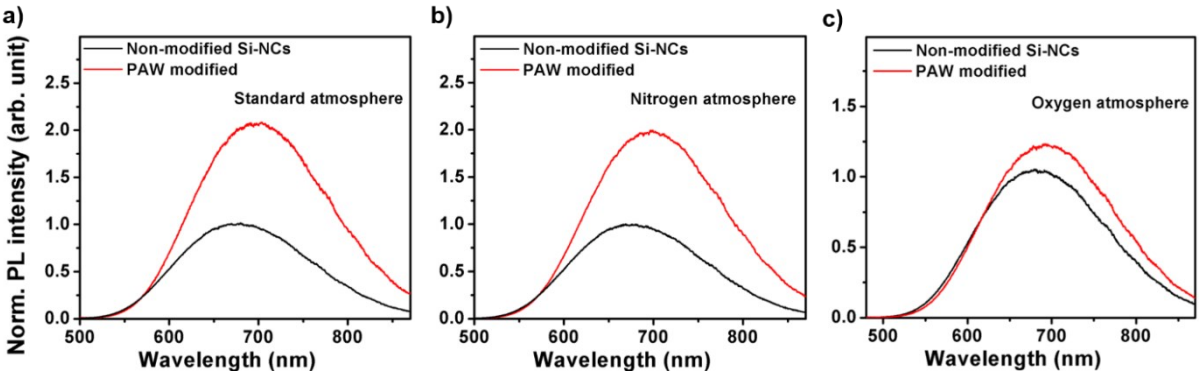

Figure S6. Comparison of normalized photoluminescence spectra of the sample Si-NCs A before and after PAW modification at different closed atmospheres. PAW with Si-NCs were plasma modified at closed atmospheres composed of a) standard atmosphere, b) nitrogen atmosphere and c) oxygen atmosphere. Chemical analysis of PAWs prepared at each atmospheres are displayed in **Table S1**. Water was activated for 30 minutes. Photoluminescence was excited at 442 nm by continuous beam of 2.7 mW. All spectra are corrected for the sensitivity of the whole detection system.

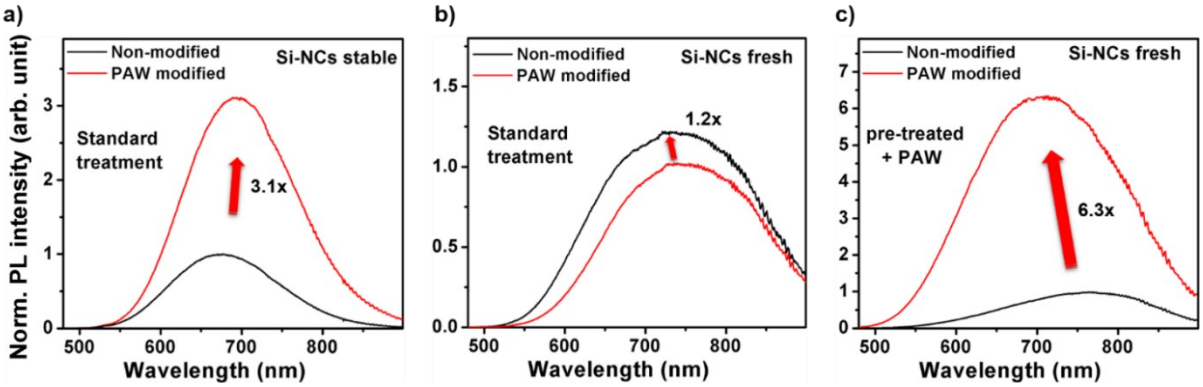

Figure S7. Comparison of PL spectra of Si-NCs before and after PAW treatment using M2 or M3 method a) PL spectra of electrochemically prepared stable Si-NCs after PAW treatment using M2 method. b) PL spectra of fresh electrochemically prepared Si-NCs after PAW treatment using M2 method. c) PL spectra of electrochemically prepared fresh Si- after PAW treatment using M3 method. Spectra are after presented after a stable state was reached. Photoluminescence was excited at 442 nm by continuous beam of 2.7 mW. All spectra are corrected for the sensitivity of the whole detection system.

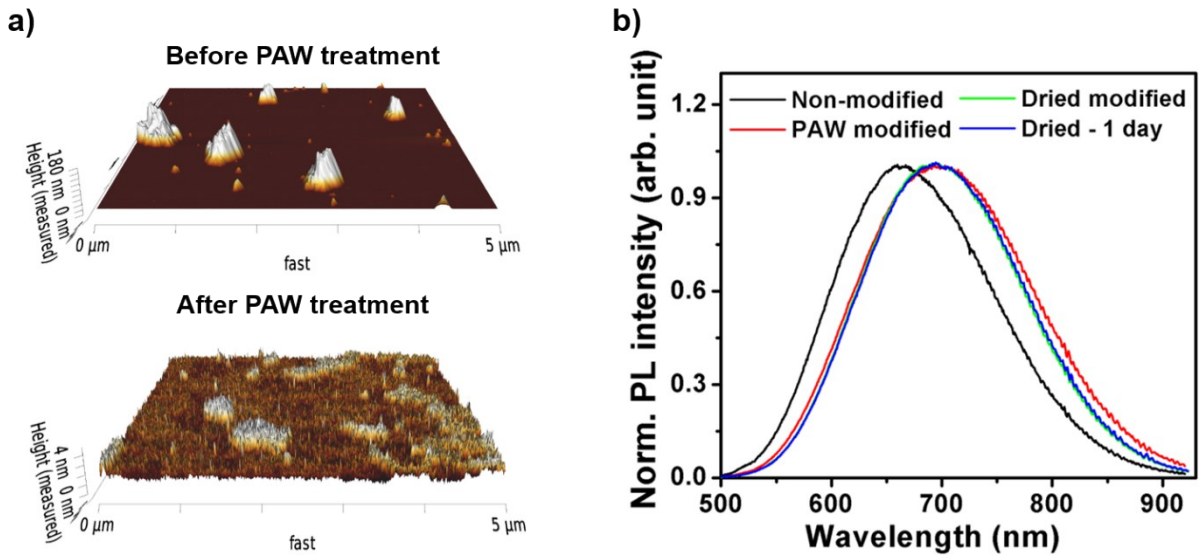

Figure S8. a) 3D picture of Si-NCs B before and after the modification by PAW obtained using atomic force microscopy. b) Normalized photoluminescence spectra of sample Si-NCs A before modification, after modification by PAW using method M2, after a drying procedure and 1 day after drying. Photoluminescence was excited at 442 nm by a continuous beam of 2.7 mW. All spectra are corrected for the sensitivity of the whole detection system.

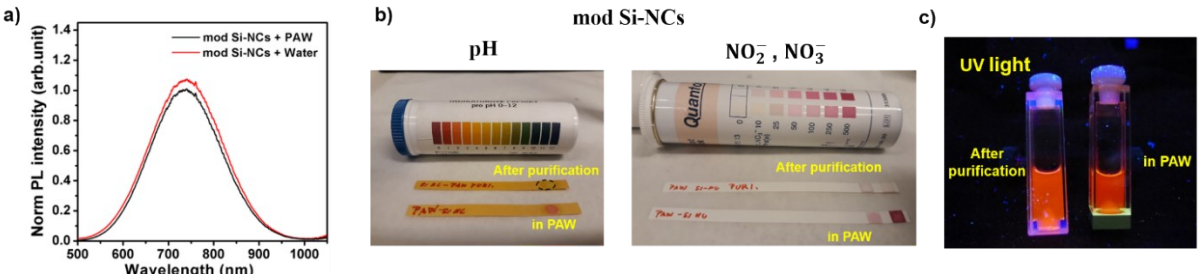

Figure S9. a) Comparison of PL spectra of non-thermal plasma synthesized Si-NCS in PAW prepared by M2 (mod Si-NCs + PAW) and the same colloidal sample after its purification using dialysis tubing (resulting pH 6). b) pH and concentration of NO_2^- and NO_3^- before and after purification. In contrast to the original sample, the purified sample showed pH 6, no NO_2^- radicals and about 1 mM of NO_3^-, which corresponds to about 1% of the original value. c) Photo of samples described in a) and b) under UV light proving similar dispersibility of the nanocrystals before and after purification.

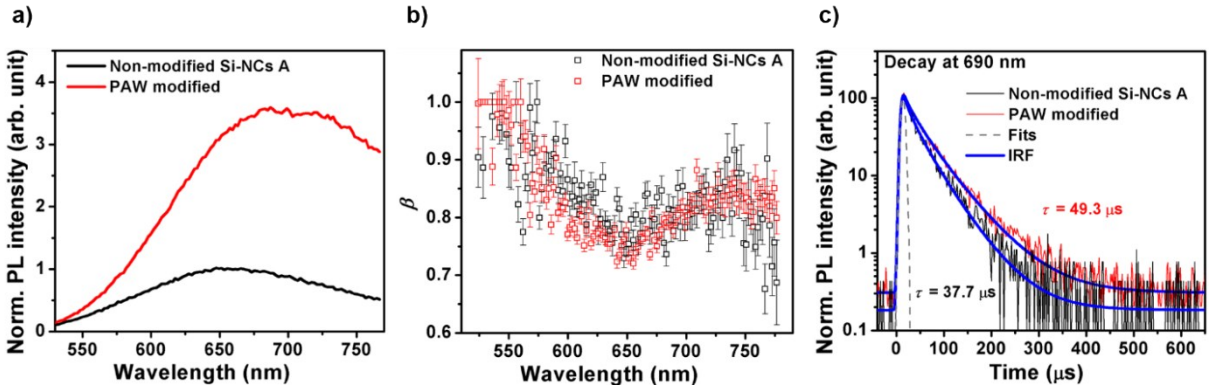

Figure S10. a) Photoluminescence spectra of the sample Si-NCs A before and after the PAW modification (method M2) obtained by the time-resolved measurements using a streak camera. b) The spectral dependence of parameter β of the stretch – exponential function used to describe the time decay of photoluminescence presented in a). c) Time-resolved photoluminescence decay of the non-modified Si-NCs A and after its modification by PAW observed at 690 nm. The solid line (labelled as fits) are the best stretch – exponential approximation of the observed days. Related photoluminescence lifetimes are indicated. IRF of the system at the used time window is displayed. The PL was excited by the laser pulses at 343 nm. The repetition frequency of the pulses was 1 kHz and the time duration of the pulses was approximately 200 fs.

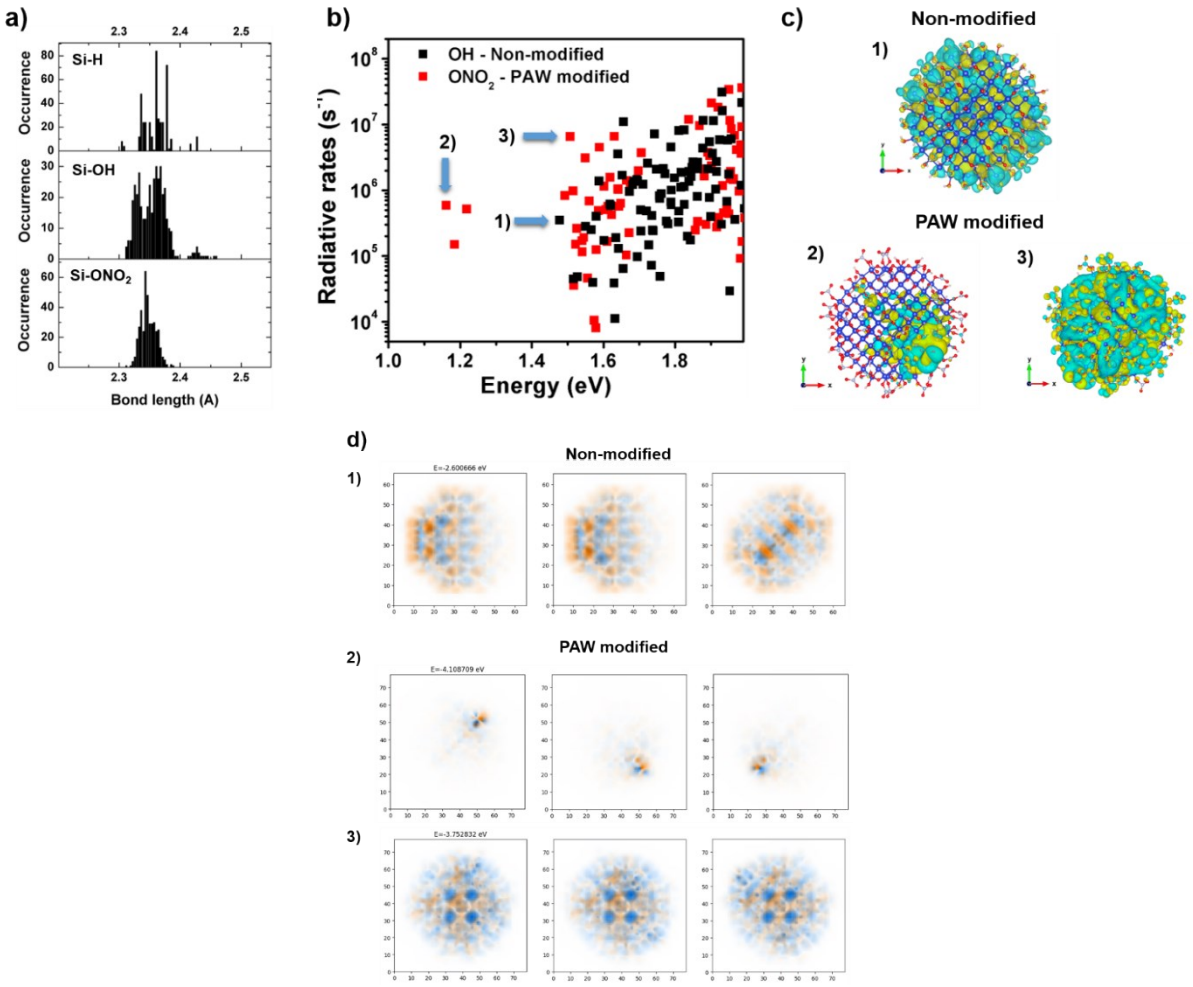

Figure S11. a) Calculated distribution of Si-Si bond length through Si-NCs nanocrystal having surface termination of Si-H, Si-OH and Si-ONO_2. b) Calculated zero-temperature radiative rates of non-modified Si-NCS (represented by partly oxidized Si surface) and PAW-modified Si-NCS (represented by partly terminated surface by NO_2 functional group bonded to silicon through oxygen atom) related to the transition between displayed energy level and highest occupied molecular level (HOMO). c) 3D visualization of electron wave function spatial distribution at three different states of Si-NCs nanocrystals (highlighted in b)). d) Projection of 3D visualization from c) to standard axis. The theoretical calculations suggest that a few highly surface-localized states basically inside the energy gap emerge as a result of the NO_2-based surface passivation (panels b, c2 and d2). These states are not taken into account in the main text simply because they are too far from the conduction band, to which the excitation of electrons occurs. The excited electrons are unable to relax into these in-gap states because of the lack of available energy-conserving phonons (phonon bottleneck) and therefore they are not relevant to the optical experiments presented in the main text. Were these states to be detected experimentally, resonant excitation and detection with low-energy photons (1000 nm or more) would be necessary.

Table S1. Chemical analysis of plasma activated water using transient spark discharge using sealed container generated at ambient conditions, nitrogen and oxygen atmosphere after 30 minutes of plasma treatment. The pH of the PAW and concentration of nitrite and nitrate ions and peroxide was monitored. The PAW properties were analyzed after reaching stable state corresponding to approximately 5 minutes after modification. Increase of PL intensity of dispersed Si-NCs is also displayed.

PAW property	Oxygen	Nitrogen	Atmosphere
pH	3	1 – 2	1 – 2
NO_2^- **(μM)**	0	1100	1830
NO_3^- **(μM)**	8000	75 000	85 000
H_2O_2 **(μM)**	4000	300	0
Si PL increase	1.28x	2.02x	2.60x

Table S2. Elemental analysis of ZnO and MgO nanoparticles. Elemental analysis by energy – dispersive X-ray spectroscopy of MgO and ZnO nanoparticles before and after modification by plasma activated water using transient spark discharge and closed space container generated at ambient conditins. Displayed are ratios of Zn/O and Mg/O before and after modification and O/N radio after analysis corrected to initial values of oxygen. PAW was modified for 30 minutes and nanoparticles were kept in PAW few days before analysis. The error of the average value is calculated as standard deviation of average value.

	ZnO nanoparticles			**MgO nanoparticles**		
Area on sample	Zn/O		O/N	Mg/O		O/N
	Before	After	After	Before	After	After
1	0.90	0.17	2.61	0.56	0.19	2.01
2	0.80	0.15	2.50	0.53	0.18	2.07
3	0.87	0.16	2.70	0.50	0.20	2.00
4	0.90	0.18	2.69	0.50	0.16	1.98
5	0.89	0.18	2.55	0.55	0.19	2.02
6	0.84	0.16	2.51	0.57	0.18	1.87
7	0.90	0.19	2.64	0.54	0.18	1.97
8	0.86	0.16	2.75	0.52	0.19	2.12
9	0.88	0.16	2.52	0.53	0.2	2.10
10	0.83	0.18	2.62	0.56	0.18	2.13
Average	0.87±0.04	0.17±0.01	2.61±0.09	0.53±0.03	0.18±0.01	2.02±0.08